Journal of Electroceramics, 15, 215–221, 2005

Ni-Cu-Zn Ferrites for Low Temperature Firing: I. Ferrite Composition and its Effect on Sintering Behavior and Permeability

J. MÜRBE & J. TÖPFER*

Fachhochschule Jena, FB Werkstofftechnik, Carl-Zeiss-Promenade 2, 07745 Jena, Germany

Submitted March 24, 2005; Revised May 19, 2005; Accepted June 23, 2005

Abstract. Ni-Cu-Zn ferrites of composition $Ni_{1-x-y}Cu_yZn_xFe_2O_4$ with $0.4 \leq x \leq 0.6$ and $0 \leq y \leq 0.25$ were prepared by standard ceramic processing routes. The density of samples sintered at 900°C increases with copper concentration y. Dilatometry reveals a significant decrease of the temperature of maximum shrinkage with y. The permeability has maximum values of $\mu = 500$–1000 for $x = 0.6$. The Curie temperature is sensitive to composition and changes form about 150°C for $x = 0.6$ to $T_c > 250$°C for $x = 0.4$, almost independent on the Cu-content. A small iron deficiency in $Ni_{0.20}Cu_{0.20}Zn_{0.60+z}Fe_{2-z}O_{4-(z/2)}$ with $0 \leq z \leq 0.06$ significantly enhances the density of samples sintered at 900°C. The maximum shrinkage rate is shifted to $T < 900$°C. These compositions are therefore appropriate for application in low temperature co-firing processes. The permeability is reduced with z, hence a small $z = 0.02$ seems to be the optimum ferrite composition for high sintering activity and permeability.

Keywords: soft ferrites, Ni-Cu-Zn ferrites, high permeability, powder morphology

1. Introduction

Ni-Cu-Zn ferrites are soft magnetic materials that are used for inductive multilayer devices. Their low sintering temperature qualifies them for co-firing with internal Ag conductors, because of the melting point of silver limits the maximum sintering temperature to $T \leq 950$°C. In addition, the relatively high permeability and good performance at intermediate to high frequencies make these ferrites the preferred materials for multilayer inductor applications. The first multilayer chip inductors were developed two decades ago [1, 2]. Multilayer chip LC filters and hybrid circuit devices appeared as second generation of inductive multilayer SMD components [3].

The promising effect of Cu addition on the sintering behavior and electromagnetic properties of Ni-Zn ferrites has been known for years [4]. On the other hand, the individual compositions of Ni-Cu-Zn ferrites used for inductors vary to some extent; ferrites relative rich in Zn (31 mol% ZnO) [5], with intermediate (26 mol% ZnO) [2] or low Zn-concentrations (15.5 mol% ZnO) [6] were proposed. Although there have been many studies in the last years focusing on ferrite powder morphology and preparation of dense microstructures with large permeability, there are only few reports on correlations between composition and properties of Ni-Cu-Zn ferrites. For example, Low et al. [7] reported on property-composition diagrams of sol-gel derived samples with 50 mol% Fe_2O_3 and Murthy [8] studied the series $Ni_{0.65-x}Cu_xZn_{0.35}Fe_2O_4$. As shown in some studies, a small deficiency of iron (<50 mol% Fe_2O_3; compositions are named sub-stoichiometric, whereas the term stoichiometric here refers to ferrites with 50 mol% Fe_2O_3 or $MeFe_2O_4$) seems to be beneficial for optimizing the shrinkage and densification of Ni-Cu-Zn ferrites [4–6]. To our knowledge no systematic study on the effect of composition on the sintering behavior and electromagnetic properties of Ni-Cu-Zn ferrites has been published. We report here the results of a systematic variation of the composition of Ni-Cu-Zn ferrites. The effects of (i) substitution of Cu for Ni in Ni-Zn ferrites with different Ni/Zn-ratio and (ii)

*To whom all correspondence should be addressed. E-mail: joerg.toepfer@fh-jena.de

iron deficiency on the sintering and densification characteristics as well as on the magnetic properties were studied.

2. Experimental

Ferrite powders of composition $Ni_{1-x-y}Cu_yZn_xFe_2O_4$ with $0.4 \leq x \leq 0.6$ and $0 \leq y \leq 0.25$ (series A ($x = 0.4$), B ($x = 0.5$) and C ($x = 0.6$)) and $Ni_{0.20}Cu_{0.20}Zn_{0.60+z}Fe_{2-z}O_{4-(z/2)}$ with $0 \leq z \leq 0.06$ (series D) were prepared by the standard ceramic route. Iron oxide (TKS Germany, grade HP) with a specific surface $S = 4.3$ m^2/g; NiO (Inco, Black Nickel Oxide, Grade F) with S = 70 m^2/g; CuO p. A. (Merck) with S = 4.6 m^2/g and ZnO (Harzsiegel Heubach, Germany, standard grade) with S = 4.5 m^2/g were used as starting materials. The oxides were wet mixed for 12 hours in a polyethylene container. The dried powders were calcined at 750–1200°C for 2 hours. Next, the powders were wet milled in a planetary ball mill to a particle size of $d_{50} = 0.6$ μm. The powders were uniaxially compacted using polyvinyl-alcohol as binder to give pellets for sintering studies or toroids for permeability measurements. The specimens were sintered at 900–1100°C for 2 hours.

The phase formation was evaluated with X-ray powder diffractometry (Siemens D5000). The powder particle size was measured using a laser diffraction system (Malvern Mastersizer 2000). The bulk density of sintered samples was determined from the dimensions and weight. Shrinkage measurements were made with a NETSCH DIL402 dilatometer on cylindrical compacts during heating to 1000–1200°C with 4 K/min heating rate. The microstructure of the samples was studied with microscopy (Zeiss DSM940A).

The magnetization was measured on powdered samples with a Quantum Design MPMS SQUID magnetometer. The magnetization was recorded in fields up to 50 kOe at 5 and 300 K and the values at maximum field were taken as saturation magnetization M_s.

The permeability of toroids (13 mm outer diameter, 6.5 mm inner diameter, 3 mm thickness) was measured with an impedance analyzer from 1 to 1000 kHz. For frequencies of up to 2 GHz permeability measurements were performed using an Agilent E4991A impedance/materials analyzer.

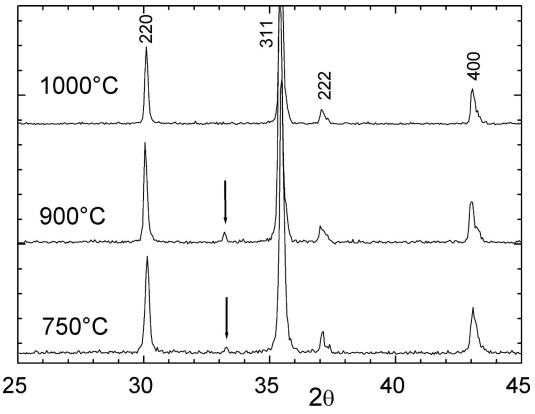

Fig. 1. XRD plots of powders of nominal composition $Ni_{0.30}Cu_{0.10}Zn_{0.60}Fe_2O_4$ calcined at temperatures of 750, 900 and 1000°C (arrows mark peaks of haematite).

3. Results and Discussion

3.1. Phase Formation

The mixed raw materials were calcined at different temperatures between 750–1000°C for 2 hours. The formation of the spinel ferrite phase was studies with XRD. For samples of the series A–C, at 750°C only compositions with $x = 0.6$ and $y \geq 0.20$ led to a single phase spinel, residual haematite peaks were observed in all other samples (Fig. 1). Ferrites with low Cu and Zn contents require higher temperatures for complete spinel formation. For example, calcination at 900°C leads to single phase ferrites for $x = 0.4$ and $y = 0.25$; for $x = 0.5$ and $y \geq 0.15$; for $x = 0.6$ and $y \geq 0.15$. Annealing at 1000°C results in complete ferrite formation for all compositions, except for $Ni_{0.6}Zn_{0.4}Fe_2O_4$ ($x = 0.4$ and $y = 0$) where a single spinel phase was finally observed after calcination at 1200°C for 2 hours. Samples of series D form ferrite spinels already after calcination at 750°C for 2 hours. This demonstrates that the phase formation is completed at lower temperatures in copper-rich and sub-stoichiometric compositions.

The lattice constants of ferrites of the three compositional series A–C were measured on samples obtained after calcination at 1000°C (except $x = 0.4$ and $y = 0$: 1200°C). The variation of a_0 with composition points at two trends (Fig. 2): (i) the lattice parameter a_o increases with the Zn-concentration x. This confirms results from earlier studies which had shown, that in Ni-Zn ferrites the unit cell size linearly increases with the Zn-content

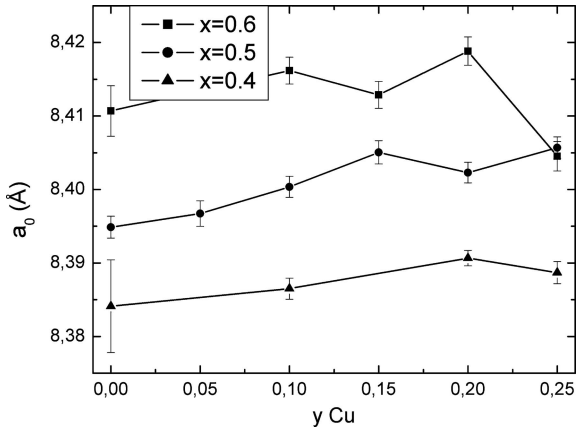

Fig. 2. Lattice constant a_0 as function of Cu-concentration y for $Ni_{1-x-y}Cu_yZn_xFe_2O_4$ with $x = 0.4$, 0.5 and 0.6.

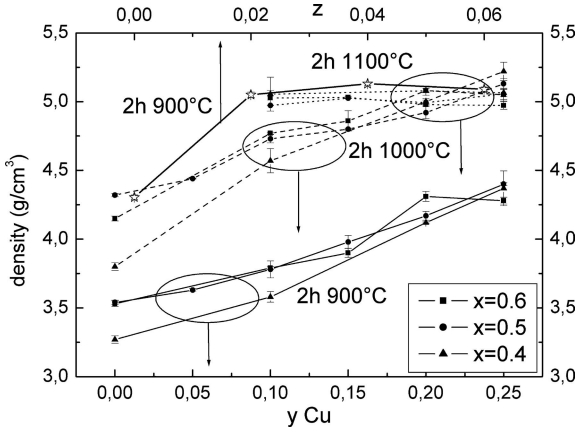

Fig. 3. Density of samples $Ni_{1-x-y}Cu_yZn_xFe_2O_4$ (series A–C) sintered at 900°C (solid lines), 1000°C (dashed lines) and 1100°C (dotted lines) for 2 hours as function of the Cu-concentration y for various Zn concentrations ($x = 0.4$, 0.5 and 0.6) and of samples $Ni_{0.20}Cu_{0.20}Zn_{0.60+z}Fe_{2-z}O_{4-(z/2)}$ (series D) with $0 \leq z \leq 0.06$ sintered at 900°C for 2 hours (star symbols and solid lines) as function of z.

[9, 10]. This is consistent with the cation distribution model of Ni-Zn ferrites $Zn_xNi_{1-x}Fe_2O_4$ [9, 10]:

$$Zn_x^{2+}Fe_{1-x}^{3+}\left[Ni_{1-x}^{2+}Fe_{1+x}^{3+}\right]O_4 \qquad (1)$$

Although Ni^{2+} on B-sites are replaced by smaller Zn^{2+} on A-sites, simultaneously Fe^{3+}-ions from A-sites are shifted into B-positions leading to an overall increase of the unit cell volume. (ii) a_0 slightly increases with the Cu-concentration y. If we assume that Ni^{2+} is replaced by Cu^{2+} on octahedral sites:

$$Zn_x^{2+}Fe_{1-x}^{3+}\left[Ni_{1-x-y}^{2+}Cu_y^{2+}Fe_{1+x}^{3+}\right]O_4 \qquad (2)$$

the larger size of Cu^{2+} (0.73 Å vs. 0.69 Å for Ni^{2+} [11]) accounts for this variation.

3.2. *Sintering Behavior*

Ferrite powders obtained by calcination at 750°C for 2 hours and subsequent fine-milling were used for all further studies. Compacts made from these powders were sintered at 900, 1000 and 1100°C for 2 hours. The density of the sintered compacts as a function of Cu-concentration y is shown in Fig. 3. The substitution of Cu for Ni promotes the densification of the ferrites. The density of the sintered samples increases with y, but sintering at 900°C generally results in low densities (about 65–83%). For samples sintered at 1000°C acceptable values of 5 g/cm^3 are observed for $y \geq 0.2$. Compared to Cu-free Ni-Zn ferrites the density of Ni-Cu-Zn ferrites is increases by up to 20%. Samples sintered at 1100°C also have a density of about 5 g/cm^3.

A significant enhancement of densification is observed for sub-stoichiometric ferrites (<50 mol% Fe_2O_3). Already a small Fe deficiency of $z = 0.02$ boosts the density of specimens sintered 2 h at 900°C to 95%; on further increase of z (series D) the density remains almost constant (Fig. 3).

Dilatometric measurements exhibit an interesting variation of the shrinkage and shrinkage rate for different compositions. As an example, Fig. 4(a) shows the effect of Cu-substitution for $x = 0.6$. Starting from $Ni_{0.4}Zn_{0.6}Fe_2O_4$ with a maximum shrinkage rate at about 1075°C the shrinkage is shifted to lower temperature with increasing y. For $x = 0.6$ and $y = 0.25$ the temperature of maximum shrinkage rate is reduced to 975°C. This trend seems to be even more pronounced for compositions with less Zn (e.g. $x = 0.4$), here the temperature of maximum shrinkage rate drops from 1175°C for $y = 0$ to 990°C for $y = 0.25$ (Fig. 4(c)). For sub-stoichiometric compositions (i.e. less than 50 mol% Fe_2O_3) the maximum shrinkage rate is shifted to even lower temperatures. For samples D, i.e. $Ni_{0.20}Cu_{0.20}Zn_{0.60+z}Fe_{2-z}O_{4-(z/2)}$ with $0 \leq z \leq 0.06$, the main shrinkage appears at $T < 900$°C for $z = 0.02$ compared to 980°C for $z = 0$

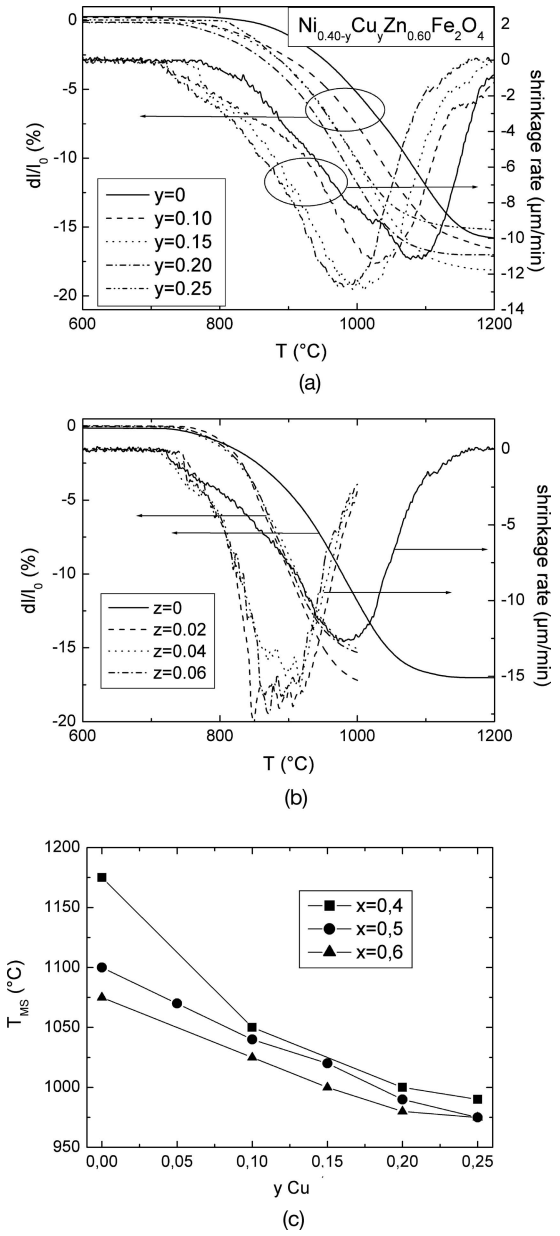

Fig. 4. Relative shrinkage and shrinkage rate (heating rate 4 K/min) of compacts made from ferrite powders of $Ni_{0.4-y}Cu_yZn_{0.6}Fe_2O_4$ with different values of y (a), of samples $Ni_{0.20}Cu_{0.20}Zn_{0.60+z}Fe_{2-z}O_{4-(z/2)}$ with $0 \leq z \leq 0.06$ (b) and variation of the temperature of maximum shrinkage rate T_{MS} with Cu-concentration for $Ni_{1-x-y}Cu_yZn_xFe_2O_4$ (c).

(Fig. 4(b)). Samples with $z = 0.04$ and 0.06 behave very similarly. Consequently, these ferrites are preferred for LTCC-type processes with a sintering temperature $T \leq 900°C$.

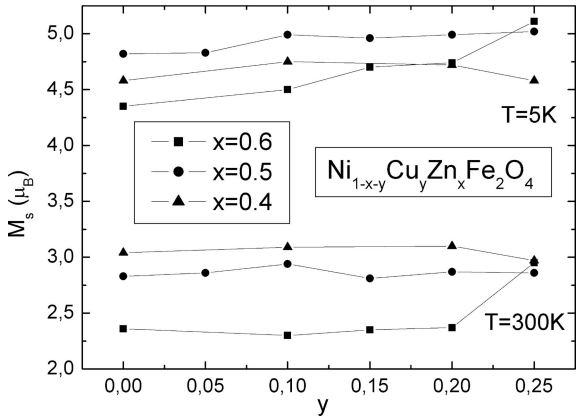

Fig. 5. Saturation magnetization as function of Cu-concentration y for $Ni_{1-x-y}Cu_yZn_xFe_2O_4$ with $x = 0.4$, 0.5 and 0.6 at 5 K and 300 K.

3.3. Magnetic Properties

The saturation magnetization of the ferrites was measured at 5 K and room temperature for various Cu concentrations y (Fig. 5). The powders used for M_s measurements were calcined at the temperatures required for the formation of a single ferrite phase; i.e. at 900°C or 1000°C (see 3.1.) and at 1200°C for $x = 0.4$ and $y = 0$. The saturation magnetization at 5 K of Ni-Zn ferrites ($y = 0$) has a maximum for $x = 0.5$ with reduced M_s for $x = 0.4$ and 0.6. This is in agreement with classic studies by Gorter [12]. Introduction of Cu does not significantly effect the saturation magnetization of Ni-Zn ferrites.

Toroids for permeability measurements were sintered at 1100°C in order to guarantee a sufficiently large and comparable density of all samples (5.02 ± 0.04 g/cm^3, Fig. 3). The microstructures of the samples sintered at 1100°C for 2 hours consists of grains of 5–10 μm in size (Fig. 6). Because all samples have almost identical microstructures the effects of grain size and porosity on the permeability have been neglected in the following discussion. The frequency variation of the permeability up to 1 MHz for $Ni_{1-x-y}Cu_yZn_xFe_2O_4$ (series A–C) shows that the samples with $x = 0.6$ have large permeabilities (Fig. 7). Substitution of Cu for Ni has a moderate effect on the permeability μ (Fig. 8). Since for $x = 0.4$ and 0.5 μ is almost independent of the Cu-content y the permeability for ferrites with $x = 0.6$ goes through a maximum at $y = 0.15$–0.20 before it becomes reduced for $y > 0.2$. The irregular

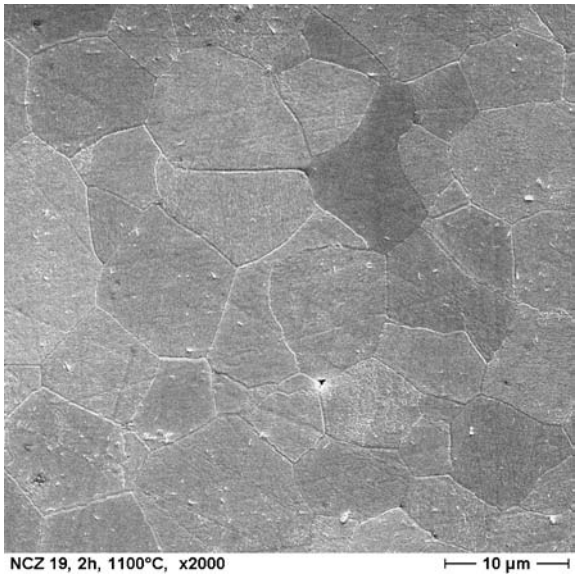

Fig. 6. SEM-micrographs of ferrites $Ni_{0.20}Cu_{0.20}Zn_{0.60}Fe_2O_4$ sintered at 1100°C for 2 hours.

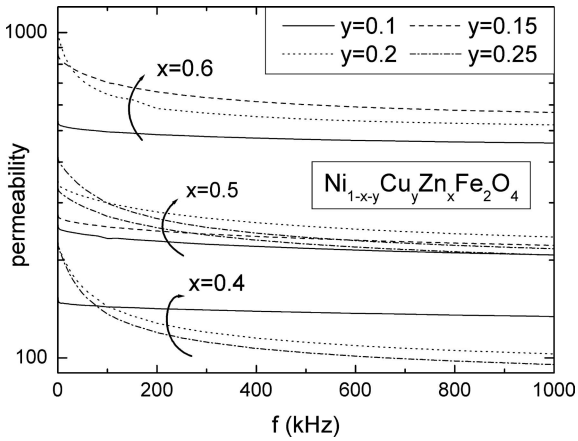

Fig. 7. Permeability as function of frequency for ferrites $Ni_{1-x-y}Cu_yZn_xFe_2O_4$ with $x = 0.4$, 0.5 and 0.6.

behavior observed for $Ni_{0.15}Cu_{0.25}Zn_{0.6}Fe_2O_4$ has already appeared in the variation of the lattice parameter (small a_0 for $y = 0.25$) and saturation magnetization (high M_s for $y = 0.25$). These features might signal a change in the cation distribution for $x = 0.6$ and $y > 0.2$.

The frequency dispersion of the permeability for Ni-Cu-Zn ferrites $Ni_{1-x-y}Cu_yZn_xFe_2O_4$ with $0.4 \leq x \leq 0.6$ and $0 \leq y \leq 0.25$ (series A–C) reveals interest-

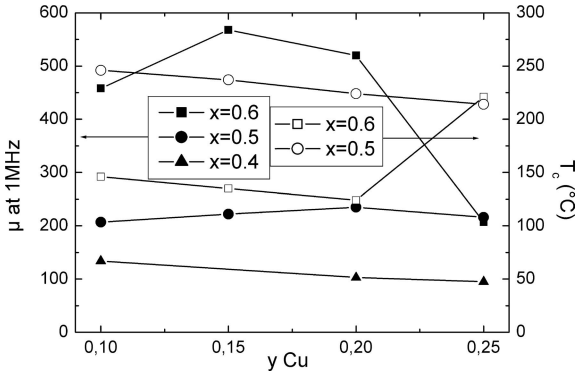

Fig. 8. Permeability at 1 MHz (full symbols) and Curie temperature T_c (open symbols) for ferrites $Ni_{1-x-y}Cu_yZn_xFe_2O_4$ with $x = 0.4$, 0.5 and 0.6.

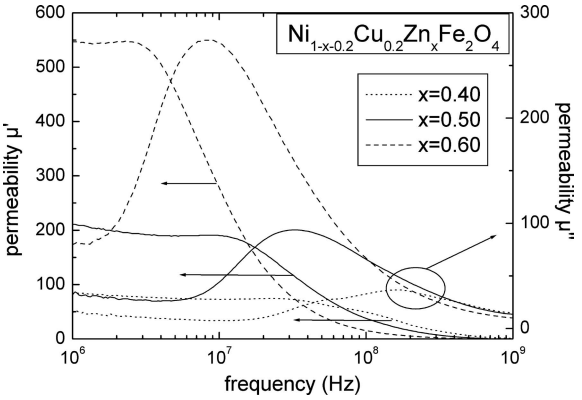

Fig. 9. Frequency dispersion of permeability for ferrites $Ni_{0.8-x}Cu_{0.2}Zn_xFe_2O_4$ with $x = 0.4$, 0.5 and 0.6.

ing effects that are related to the ferrite composition. As an example the real and imaginary parts of the permeability in the frequency range from 1–1000 MHz for the compounds $Ni_{0.8-x}Cu_{0.2}Zn_xFe_2O_4$ are shown in Fig. 9. The following characteristics of the curves are to be noticed: (i) as discussed before, the absolute values of the real part of the permeability μ' at 1 MHz decrease with decreasing Zn content x. (ii) the frequency variation of μ' reveals a decay of the permeability beginning at 3 MHz for $x = 0.6$, at 20 MHz for $x = 0.5$ and at 50 MHz for $x = 0.4$. Simultaneously, the imaginary part of the permeability μ'' has a maximum at 8; 35 and 200 MHz for $x = 0.6$; 0.5 and 0.4, respectively. These findings fit to expectations: according to Snoek's law the resonance frequency is shifted toward higher frequencies for ferrites with lower permeability. Nakamura [13] has analyzed the complex

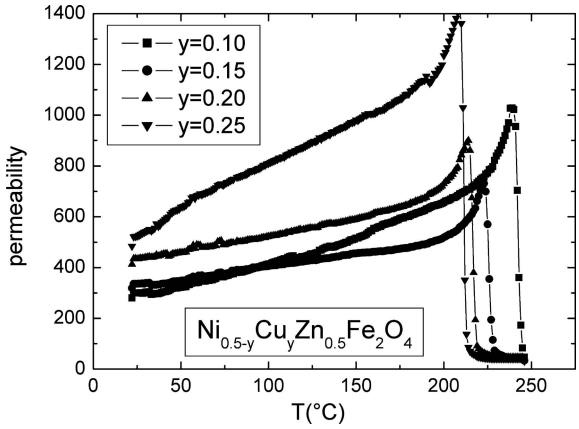

Fig. 10. Permeability as a function of temperature for ferrites $Ni_{0.5-y}Cu_yZn_{0.5}Fe_2O_4$ with $0.1 \leq y \leq 0.25$.

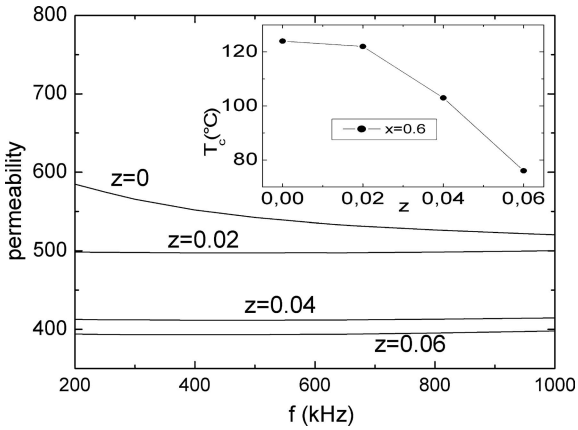

Fig. 11. Permeability as function of frequency for ferrites $Ni_{0.20}Cu_{0.20}Zn_{0.60+z}Fe_{2-z}O_{4-(z/2)}$ with $0 \leq z \leq 0.06$; inset: Curie temperature vs. z.

permeability spectra of Ni-Cu-Zn ferrites in detail and concluded that both domain wall displacement and spin rotation contribute to the permeability at a frequency below 10 MHz. This demonstrates that the choice of ferrite composition is essential if the maximum operational frequency of the inductor is an important issue.

The Curie temperature T_c is another property which is relevant for inductor applications and which is very sensitive to composition. The variation of permeability with temperature is shown for $Ni_{0.5-y}Cu_yZn_{0.5}Fe_2O_4$ in Fig. 10; the permeability vanishes at T_c. The Curie temperature as a function of the Cu-concentration y of Ni-Cu-Zn ferrites of series B ($x = 0.5$) and C ($x = 0.6$) is shown in Fig. 8, T_c increase with decreasing Zn content x. The values for $x = 0.4$ are not included in Fig. 8; T_c of these ferrites is above the maximum measuring temperature of 250°C. With increasing copper concentration y a slight decrease of T_c is observed (except for $x = 0.6$ and $y = 0.25$).

The permeability of the sub-stoichiometric ferrites $Ni_{0.20}Cu_{0.20}Zn_{0.60+z}Fe_{2-z}O_{4-(z/2)}$ displays a significant reduction of μ with increasing iron deficiency z (Fig. 11). Simultaneously, the Curie temperature also decreases with z (Fig. 11, inset). This demonstrates that z should be small in order to not deteriorate the permeability properties of the inductor material.

4. Conclusions

The integration of Cu into Ni-Zn ferrites drastically effects the densification and sintering behavior. The density after sintering at 900 and 1000°C of $Ni_{1-x-y}Cu_yZn_xFe_2O_4$ increases with the Cu-content y. The temperature of maximum shrinkage is reduced to about 980°C for $y = 0.25$. If, in addition, the iron content is reduced, i.e. $Ni_{0.20}Cu_{0.20}Zn_{0.60+z}Fe_{2-z}O_{4-(z/2)}$ with $0 \leq z \leq 0.06$, the temperature of maximum shrinkage rate is shifted to $T < 900$°C and high densities are observed after sintering at 900°C. The permeability and the Curie temperature are sensitive to composition: ferrites with $x = 0.6$ and $y \leq 0.2$ show large permeabilities, for $x = 0.5$ and $x = 0.4$ the permeability is decreased. For $x = 0.4$ and 0.5 the Cu-content y has only minor effect on the permeability, in the case of $x = 0.6$ μ has a maximum at $y = 0.15$–0.20 and decreases at $y > 0.2$. T_c can be tailored from 150 to >250°C by choosing x and y. Reduction of the iron content z further reduces μ.

Ni-Cu-Zn ferrites for multilayer inductors have compositions with less than 50 mol% Fe_2O_3 to facilitate sintering at 900°C. On the other hand, the degree of iron deficiency is small (e.g. $z \approx 0.02$) to ensure the permeability of the inductor material.

Acknowledgments

The authors thank the Bundesministerium für Bildung und Forschung (Germany) for financial support (grant 03WKF03A). We acknowledge the contributions of Mrs. M. Friedrich (FHJ) for SEM and Mr. V. Döhnel (Tridelta GmbH) for permeability measurements.

References

1. T. Nomura and A. Nakano, in *Proceedings of the Sixth International Conference on Ferrites (ICF6)*, Tokyo, 1198 (1992).
2. T. Nakamura and Y. Okano, *J. Phys. IV France*, **7**, C1-91 (1997).
3. K. Yasuda, Y. Mochizuki, and M. Takaya, in *Proceedings of the Eight International Conference of Ferrites (ICF8)*, Kyoto, 1162 (2000).
4. J.H. Nam, H.H. Jung, J.Y. Shin, and J.H. Oh, *IEEE Trans. Magn.*, **31**, 3985 (1995).
5. S.C. Byeon, H.J. Je, and K.S. Hong, *Jpn. J. Appl. Phys.*, **36**, 5103 (1997).
6. A. Nakano and T. Nomura, *Ceram. Transactions*, **97**, 285 (1999).
7. K.O. Low and F.R. Sale, *J. Magn. Magn. Mater.*, **256**, 221 (2003).
8. S.R. Murthy, *J. Mater. Sci. Lett.*, **21**, 657 (2002).
9. J.M. Daniels and A. Rosencwaig, *Canad. J. Phys.*, **48**, 381 (1970).
10. A.M. El-Sayed, *Ceramics Intl.*, **28**, 363 (2002).
11. R.D. Shannon, *Acta Cryst.* A**32**, 751 (1976).
12. E.W. Gorter, *Philips Res. Repts.*, **9**, 321 (1954).
13. T. Nakamura, *J. Magn. Magn. Mater.*, **168**, 285 (1997).